J. Chem. Thermodynamics xxx (2017) xxx–xxx

Contents lists available at ScienceDirect

J. Chem. Thermodynamics

journal homepage: www.elsevier.com/locate/jct

Phase equilibria, kinetics and morphology of methane hydrate inhibited by antifreeze proteins: application of a novel 3-in-1 method

Lisa U. Udegbunam [a], James R. DuQuesnay [a], Laura Osorio [a,b], Virginia K. Walker [c], Juan G. Beltran [a,*]

[a] Department of Chemistry and Chemical Engineering, Royal Military College of Canada, Kingston, ON, Canada
[b] Department of Chemical Engineering, Universidad de Los Andes, Bogota, Colombia
[c] Department of Biology, Queen's University, Kingston, Canada

ARTICLE INFO

Article history:
Received 31 May 2017
Received in revised form 10 August 2017
Accepted 11 August 2017
Available online xxxx

Keywords:
Methane hydrate
Hydrate inhibitors
Flow assurance
TmAFP
LpAFP
Maxi

ABSTRACT

The action of three distinct recombinant antifreeze proteins (AFPs) as methane hydrate inhibitors was examined using a recently-developed reactor. Compared with traditional approaches, this reactor uses minimal reactant volumes and short experimentation times to assess phase equilibria, kinetics and morphology of a hydrate system in a single experiment (3-in-1). Two of the recombinant AFPs are considered highly active with respect to the inhibition of ice: 'Maxi', a fish AFP, and a beetle AFP (TmAFP). The third protein from a grass, is classified as a low activity AFP (LpAFP). 'Maxi', an AFP that has not been tested previously as a hydrate inhibitor, slowed hydrate growth rates up to an order of magnitude compared to pure water. TmAFP and LpAFP also exhibited kinetic inhibition, but were less effective than 'Maxi'. In the presence of AFPs, hydrate films were thinner and showed a single growth mechanism compared to multiple crystal growth mechanisms observed in control experiments. The addition of TmAFP generated large irregular hydrate halos that propagated outside the original water boundary. Halo propagation was somewhat less prominent with LpAFP, and was not observed with 'Maxi'. Although, none of the AFP's showed thermodynamic inhibition properties, 'Maxi' appeared to form clusters of hydrate which remained metastable in the liquid–vapour region.

1. Introduction

Clathrate hydrates are crystalline, non-stoichiometric compounds composed of hydrogen-bonded polyhedral water cages with entrapped guest molecules such as methane, propane, or carbon dioxide. Such hydrates form at high pressures and low temperatures [1–3]. Gas hydrates are a major flow assurance concern to the oil and gas industry in deep waters and cold weather regions where they can block flow lines, and valves resulting in safety hazards and capital losses [4,1,5,6]. Traditionally, thermodynamic hydrate inhibitors (THIs) such as ethanol or glycerol have been used to shift hydrate equilibrium. However, THI dosage is in the order of 0.25 mass fraction of inhibitor in the water phase which increases recovery costs [4,3]. As well, the environmental impact from THI use has resulted in the imposition of restrictions in European sectors as well as the Arctic [7]. In response to this, industry has transitioned to low-dosage hydrate inhibitors (LDHIs; 0.001–0.01 mass fraction [4]). One class of LDHIs are kinetic hydrate inhibitors (KHIs), which are water soluble polymeric compounds such as polyvinylpyrrolidone (PVP). LDHIs delay the formation of hydrate and allow the transport of hydrocarbons even within the hydrate stability region [1].

Although effective, some LDHIs are toxic and have poor biodegradability; thus, KHIs with a reduced environmental persistence are of special interest [4]. For example, pure aminoacids have been found to act both as thermodynamic and kinetic inhibitors of methane hydrates through selective inhibition of the formation of particular cages [8]. Furthermore, antifreeze proteins have been shown to adsorb to clathrate hydrates [7] and to act as KHIs [9].

Antifreeze proteins (AFPs) produced by certain organisms, adapted to low temperature environments, adsorb to microscopic ice crystals. As a consequence, AFPs lower the freezing temperature of water which is measured as thermal hysteresis (TH), or the difference between the freezing and melting points of water [7]. AFPs are classified with respect to their various TH activities. A highly active AFP (TH of 1.4 °C at 20 μM) from the meal worm, *Tenebrio molitor* (TmAFP) folds into a 8.4 kDa right handed β-helix [10–12]. Highly active 'Maxi' AFP (TH of 1.1°C at 0.1 mg · mL^{-1}) from the winter flounder, *Pseudopleuronectes americanus*, is a 33 kDa α-helical, homodimer [13,14]. In contrast, the perennial rye grass LpAFP folds into a 13.5 kDa left-handed α-solenoid but

* Corresponding author.
E-mail address: juan.beltran@rmc.ca (J.G. Beltran).

http://dx.doi.org/10.1016/j.jct.2017.08.015
0021-9614/

has a very low TH of 0.1 °C at 1 mg · mL^{-1} [7,15]. Remarkably some AFPs, including TmAFP and LpAFP, but not 'Maxi' have been shown to adsorb to gas hydrates and to act as KHIs [10,16,17].

The non-colligative nature of AFPs makes them good candidates as a first approximation to test the 3-in-1 method developed by DuQuesnay et al. [18]. The reason for this is that the change in non-colligative inhibitor concentration, induced by crystal growth, should not alter the system behavior. Although the use of AFPs in the field is not practical currently, understanding how they interact with hydrates could lead to the development of new polymeric compounds, making them worthy candidates for study. Observing the effect AFPs have on the growth, morphology, and phase equilibrium of hydrates allows us to proceed in this direction.

The objective of this work was to test the capability of the new 3-in-1 reactor/method [18] to assess phase equilibria, morphology and kinetics of methane hydrates in the presence of inhibitors. The non-colligative nature of AFPs made them an excellent candidate for this. For the first time, we are also showing the effect on methane hydrates of the 'Maxi' AFP.

2. Experimental

2.1. Apparatus

The apparatus consists of a pressure vessel consisting of a 316 stainless steel cell with several radial ports for inlet and outlet gas lines as well as temperature and pressure monitors (Fig. 1). A High-Pressure Bilateral Temperature Control Stage (HP-BTCS) was placed inside the reactor to provide precise temperature control of the sample [18]. Two sapphire sight windows (Rayotek, CA, USA) positioned on the vertical axis of the vessel allowed illumination and visual access to the sample. Images were acquired with a PCO.edge 5.5 cMOS camera (Optikon, ON, Canada). A Schott KL2500 LCD cold light source (Optikon, ON, Canada) was used for illumination. The vessel was wrapped in a coolant jacket which consisted of a copper coil covered with two layers of insulation. The coil was cooled with a Thermo Scientific AC200 refrigerated chiller (Fisher Scientific, Canada), which circulated a 50/50 (v/v) mixture of ethylene glycol and water through the coil. The pressure of the vessel was measured with a Rosemount 3051S pressure transmitter (Laurentide Controls, QC, Canada) and temperature was monitored with a Pt RTD probe (Omega Engineering, Canada). Instrumental standard uncertainties were as follows: for bulk temperature $u_{T_{RTD}} = 0.32$ K and for pressure $u_p = 0.005$ MPa. The sample stage (HP-BTCS) controlled the temperature on opposite sides of the sample precisely and independently [18]. Both ends of the stage were equipped with a thermoelectric cooler (TE Technology, MI, USA). A sapphire slide was used to hold the water sample and bridge the two ends of the stage. Slide temperatures were measured by thermistor elements (TE Technology, MI, USA) with an instrumental standard uncertainty of $u_{T_{thermistor}} = 0.01$ K. A detailed description of the apparatus and method are available in DuQuesnay et al. [18].

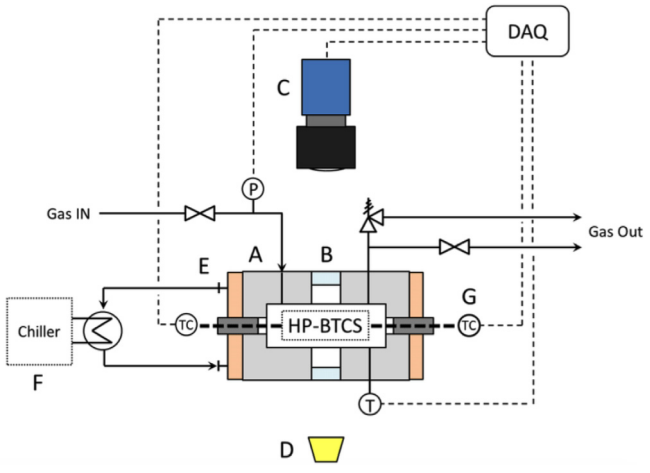

Fig. 1. Schematic of the reactor setup [18]. (A) Pressure vessel (B) Sapphire windows (C) Video camera (D) Light source (E) Cooling coil (F) Refrigerated circulator (G) Temperature controllers.

Table 1
Reagents used in this study. HEPES stands for 4-(2-Hydroxyethyl) piperazine-1-ethanesulfonic acid. Resistivity was used as an indicator of water purity: at the source, it was measured to be 18 MΩ · cm.

Chemical Name	Source	Purity	Purity Units
Distilled Water	In–house	see caption	see caption
Nitrogen	Air Liquide	99.99%	mole fraction
Methane	Air Liquide	99.99%	mole fraction
HEPES Buffer			
NaCl	Sigma–Aldrich	99.5%	mass fraction
HEPES, Sodium Salt	BioShop Canada	99.5%	mass fraction
K_2HPO_4	Sigma–Aldrich	98%	mass fraction
$CaCl_2$	Sigma–Aldrich	99.5%	mass fraction
$MgCl_2$	Sigma–Aldrich	98%	mass fraction
HCl_{aq}	Sigma–Aldrich	37%	mass fraction
$NaOH_{aq}$	Sigma–Aldrich	35%	mass fraction

Table 2
Buffer Recipe. HCl or NaOH solutions were used to adjust to pH = 7.4.

Chemical	Final Concentration	Concentration Units
NaCl	115	mM
HEPES, Sodium Salt	20	mM
K_2HPO_4	2.4	mM
$CaCl_2$	1.2	mM
$MgCl_2$	1.2	mM
H_2O	Solvent	

2.2. Methods and materials

Samples: Recombinant proteins were made and purified exactly as detailed previously [17,19]. Solutions consisted of deionized water and buffer controls and experimental solutions of 0.1 mg · mL^{-1} TmAFP in water, 0.1 mg · mL^{-1} LpAFP in water, and 0.1 mg · mL^{-1} 'Maxi' in a buffer solution. 'Maxi' is not stable in pure water, and thus required additional solutes. Each sample (20 μL) was placed on the sapphire slide with a micropipette. The vessel was sealed and initially purged with nitrogen, and then it was purged several times with methane gas. Table 1 summarizes reagent properties and Table 2 provides the buffer composition.

2.2.1. Crystal formation history

The sample was cooled to 253.15 K to form ice, in a methane atmosphere at 0.2 MPa. The pressure was increased to experimental pressure (4 MPa) upon ice formation, and the temperature was increased past 273.15 K to convert the ice to hydrate. The stage was then heated 1 K above the hydrate-liquid–vapour (H-L-V) equilibrium at experimental pressure to dissociate the hydrate and retain 'hydrate formation history' [20–23].

2.2.2. Hydrate formation and dissociation

For hydrate formation experiments the temperature and pressure surrounding the stage were maintained constant. Four minutes after the completion of the crystal formation history, the sample was cooled to experimental temperature using the HP-